COBEM 2023 27TH INTERNATIONAL CONGRESS OF MECHANICAL ENGENEERING

ABCM Brazilian Society of Mechanical Sciences and Engineering
27th ABCM International Congress of Mechanical Engineering
December 04-08, 2023, Florianópolis-SC, Brazil

COB-2023-1522
COMPARISON OF CONTROL TECHNIQUES APPLIED TO AN ELECTROMAGNETIC LEVITATION SYSTEM BY ATTRACTION

Renan Imamura Marques
Éverton Lins de Oliveira
Mauá Institute of Technology (IMT), University of São Paulo (USP)
renan_imamura@maua.br, ev_lins@usp.br

Décio Crisol Donha
University of São Paulo (USP)
decdonha@usp.br

Abstract. *This paper describes the design and construction of a prototype of an electromagnetic attraction system for the levitation of small ferromagnetic objects. The electromagnetic levitation system is chosen because it is a highly nonlinear unstable open loop device, frequently used as control benchmark. Also, this system has a wide range of applications, such as the handling of small objects in clean rooms present in the food production, pharmaceutical and electronic industries as well in the scientific area. The objective of the work is to apply different control techniques to a prototype, obtaining experimental data for performance analysis of each alternative. Following the historical evolution of control techniques, classical controllers are initially applied, in a single input single output approach. Among these techniques, phase lead and lead-lag control are implemented. Next, other control techniques such as Proportional-Integral-Derivative (PID), Linear Quadratic Regulator (LQR) and H-Infinity are numerically applied for comparison purpose. The paper presents the mathematical modeling of the system, the synthesis and implementation of the controllers, the practical experiments and the analysis of the performance of each control proposed. It also presents the build of the prototype, including the power electromagnet instrumented with optical sensors used to measure the air gap distance (distance between the levitated object and the electromagnet core). Robustness issues are also in sight, since system parameters, such as the electrical resistance of the electromagnet, can change during operation.*

Keywords: *electromagnetic levitation, Lead-Lag, PID, LQR, H-Infinity.*

1. INTRODUCTION

Electromagnetic levitation is a technology that has been the subject of study and research in various fields, including physics, engineering, and control systems. According to (Kumar et al., 2022), electromagnetic levitation systems are a promising field that brings alternative methods for moving objects without contact. In the electronics and pharmaceutical industries, electromagnetic levitation is used to manipulate small objects in clean rooms, where the presence of particles is minimized to ensure product quality.

Due to being an unstable and nonlinear system, electromagnetic levitation is a classic system for applying control techniques in the academic environment. (Goel & Swarup, 2016) developed a super-twisting sliding mode control for a magnetic levitation system. In the numerical simulations, the controller guarantees finite-time reachability, effective disturbance rejection and continuous control without chattering. (Yaseen & Abd, 2018) evaluated the performance of Linear-Quadratic Regulator (LQR), Proportional-Integral-Derivative (PID), and *phase lead* controllers for a levitation system consisting of an acrylic base sustained by the attraction between four electromagnets and neodymium magnets. They found that the LQR controller performed better than other control techniques. (Abubakar et al., 2019) presented an H-Infinity control for a magnetic levitation system. The controller was synthesized based on the mixed sensitivity method. In the numerical simulations, the H-Infinity compensator provides improved performance and robustness compared to a proportional-integral-velocity controller with feedforward. (Majewski et al., 2022) developed a hybrid fuzzy logic PID and feedforward neural network regulators for the magnetic levitation problem. The numerical simulations with the artificial intelligence approaches have outperformed the classical ones in the context of control accuracy and control speed.

This work presents the development of modeling and control of an electromagnetic levitation system for small ferromagnetic objects. Two compensators based on the classic control techniques (single input and single output) using a *phase lead* and lead-lag structure are proposed and experimentally verified. Other controllers such as PID, LQR and H-Infinity control are tested through numerical simulation. The article is organized as follows: Section 2 describes the elements that make up the electromagnetic levitator; Sections 3 and 4 describe the development of the mathematical model and system analysis, respectively; Section 5 describes the development of the controllers; practical results are presented in Section 6; conclusions are presented in Section 7.

2. SYSTEM ELEMENTS

The prototype consists of an 18 W electromagnet, wound with 22 AWG enameled copper wire, steel core, an optical sensor used to measure the air gap distance, a full bridge drive, model *LM298*, to activate the of the electromagnet and a control board, *NI myRIO*. The schematic of the system elements is presented in Figure 1.

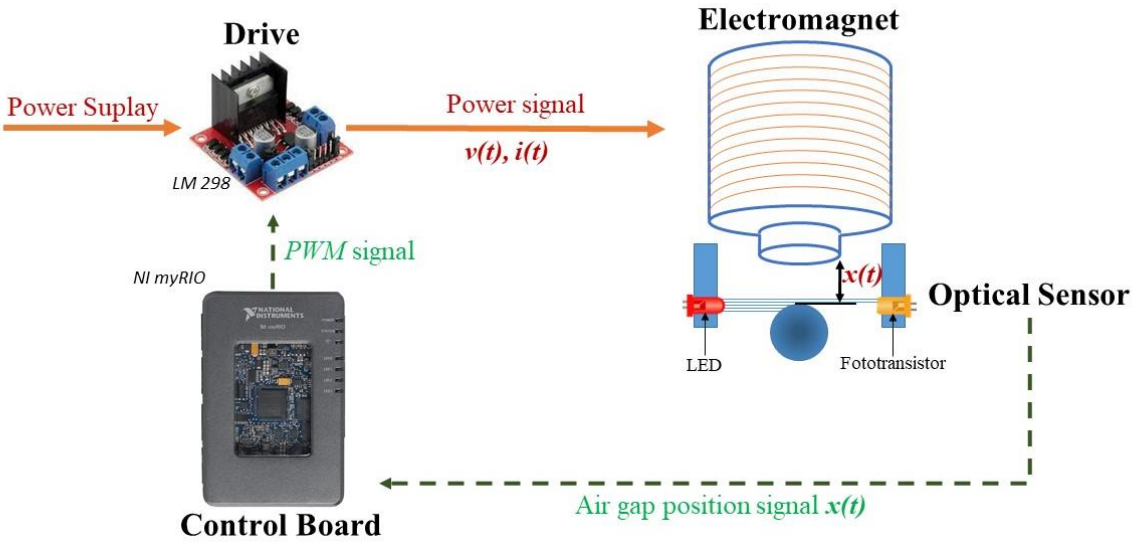

Figure 1. Prototype schematic.

A structure made of wood was developed to fix the electromagnet and the optical sensor. The prototype is shown in Figure 2.

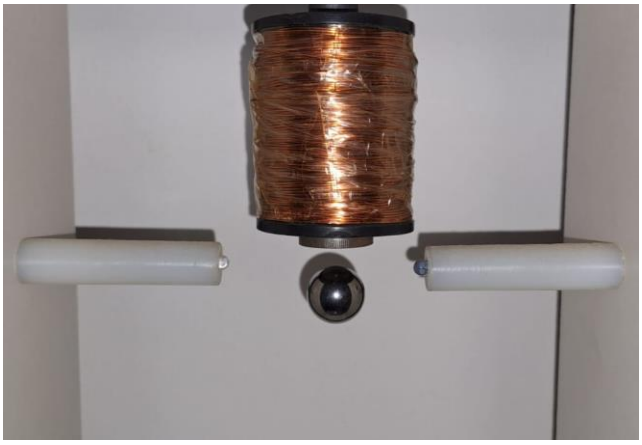

Figure 2. Electromagnetic levitator prototype.

3. SYSTEM MODEL

The system has three states, electric current circulating through the electromagnet, the air gap distance and the velocity of the levitated object. Of the three states, only the air gap distance is output from the system. The system has only one input, the voltage applied to the electromagnet terminals. As the system is non-linear, the model was linearized around the equilibrium point. The next sections describe the development of the levitator model divided into mechanical and electrical subsystems and the linearization of the model.

3.1 Mechanical subsystem

The mechanical subsystem is obtained by analyzing the forces acting on the levitated ferromagnetic object. The free-body diagram of the mechanical subsystem is shown in Figure 3, where F_g and F_m are the gravitational and magnetic forces, respectively.

Figure 3. Mechanical subsystem free body diagram.

The magnetic force generated by the electromagnet is given by:

$$F_m(t) = C\frac{i^2(t)}{x^2(t)}, \tag{1}$$

where, C is the force constant, $i(t)$ is the current in the electromagnet and $x(t)$ is the air gap distance.

The gravitational force of the ferromagnetic object is given by:

$$F_g = mg, \tag{2}$$

where, m is the mass of the ferromagnetic object and g is the acceleration due to gravity. Applying Newton's second law, comes:

$$F_g - F_m = m\frac{d^2x(t)}{dt^2}. \tag{3}$$

Substituting Eq. (1) and (2) in Eq. (3), it is obtained the equation of the mechanical system as follows:

$$mg - C\frac{i^2(t)}{x^2(t)} = m\,\frac{d^2x(t)}{dt^2}. \tag{4}$$

3.2 Electrical subsystem

The electrical circuit of the electromagnet is shown in Figure 4, where R is the electrical resistance of the electromagnet, $i(t)$ is the electric current and L is the inductance.

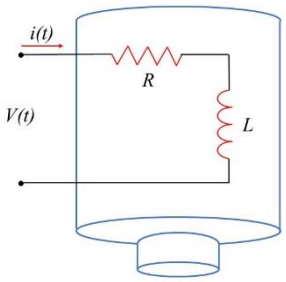

Figure 4. Electrical diagram of the electromagnet.

The *Kirchhoff* law was applied to the electromagnet circuit as follows:

$$V(t) = Ri(t) + \frac{di(t)}{dt}L. \tag{5}$$

Rearranging Eq. (4) and (5), the equations the model of the dynamic of the system is given by:

$$\begin{cases} \dot{x}(t) = v(t) \\ \dot{v}(t) = g - \frac{c}{m}\frac{i^2(t)}{x^2(t)} \\ \frac{di(t)}{dt} = -\frac{R}{L}i(t) + \frac{1}{L}V(t) \end{cases} \tag{6}$$

It is observed that the equations describing the system are non-linear. To develop the design of the controllers proposed in this article, the system must be linear considering small variations around the equilibrium point. The next section describes the linearization of the model around this equilibrium point.

3.3 System linearization

To develop the design of the controllers proposed in this article, the system is linearized considering small variations around the equilibrium point. Applying the equilibrium condition in Eq. (5), and considering the derivative of the current as a function of time equal to zero, comes:

$$V_{eq} = Ri_{eq}, \tag{7}$$

where V_{eq} and i_{eq} are respectively the voltage and electric current in the electromagnet in the equilibrium condition.

Isolating i_{eq}, comes:

$$i_{eq} = \frac{V_{eq}}{R}. \tag{8}$$

Applying the equilibrium condition in Eq. (4), where the derivative of the distance $x(t)$ as a function of time is zero, one has:

$$C\frac{i_{eq}^2}{x_{eq}^2} = mg. \tag{9}$$

Reconfiguring Eq. (11), the air gap of the ferromagnetic object at the equilibrium point may be written as:

$$x_{eq} = i_{eq}\sqrt{\frac{C}{mg}}, \tag{10}$$

or:

$$x_{eq} = \frac{V_{eq}}{R}\sqrt{\frac{C}{mg}}. \tag{11}$$

To easy the linearization procedure presentation, the state functions of the system were respectively named as f_1, f_2 and f_3 as shown below:

$$\begin{cases} \dot{x}(t) = f_1(x, v, i, V) = v(t) \\ \dot{v}(t) = f_2(x, v, i, V) = g - \frac{c}{m}\frac{i^2(t)}{x^2(t)} \\ \frac{di(t)}{dt} = f_3(x, v, i, V) = -\frac{R}{L}i(t) + \frac{1}{L}V(t) \end{cases} \tag{12}$$

The values of the partial derivatives of the function $f_1(x, v, i)$ is given by:

$$\left(\frac{\partial f_1}{\partial x}\right)_{x=x_0} = 0;\ \left(\frac{\partial f_1}{\partial v}\right)_{v=0} = 1;\ \left(\frac{\partial f_1}{\partial i}\right)_{i=i_0} = 0. \tag{13}$$

The partial derivatives values of the function $f_2(x, v, i)$ follows:

$$\left(\frac{\partial f_2}{\partial x}\right)_{x=x_0;\, i=i_0} = \frac{2Ci_0^2}{mx_0^3};\ \left(\frac{\partial f_2}{\partial v}\right)_{v=0} = 0;\ \left(\frac{\partial f_2}{\partial i}\right)_{x=x_0;\, i=i_0} = -\frac{2Ci_0}{mx_0^3}. \tag{14}$$

In the same way the partial derivatives values of the function $f_3(x, v, i)$ are given by:

$$\left(\frac{\partial f_3}{\partial x}\right)_{x=x_0} = 0;\ \left(\frac{\partial f_3}{\partial v}\right)_{v=0} = 0;\ \left(\frac{\partial f_3}{\partial i}\right)_{i=i_0} = -\frac{R}{L}. \tag{15}$$

At last, the partial derivatives values of the functions $f_1(V)$, $f_2(V)$, $f_3(V)$ are as follows:

$$\left(\frac{\partial f_1}{\partial V}\right)_{V=V_0} = 0;\ \left(\frac{\partial f_2}{\partial V}\right)_{V=V_0} = 0;\ \left(\frac{\partial f_3}{\partial V}\right)_{V=V_0} = \frac{1}{L}. \tag{16}$$

The linearized system model in state space is then:

$$\begin{bmatrix}\dot{x}\\ \dot{v}\\ \dot{i}\end{bmatrix} = \begin{bmatrix}0 & 1 & 0\\ \frac{2i_0^2C}{mx_0^3} & 0 & -\frac{2Ci_0}{mx_0^2}\\ 0 & 0 & -\frac{R}{L}\end{bmatrix}\begin{bmatrix}x\\ v\\ i\end{bmatrix} + \begin{bmatrix}0\\ 0\\ \frac{1}{L}\end{bmatrix}u, \tag{17}$$

$$y = \begin{bmatrix}1 & 0 & 0\end{bmatrix}\begin{bmatrix}x\\ v\\ i\end{bmatrix}. \tag{18}$$

The system parameters are given in Table 1.

Table 1 – System parameters

Parameters	Value	Description
$\boldsymbol{m}$	35.4 g	Mass
$\boldsymbol{R}$	5.4 Ω	Electrical resistance of the electromagnet
$\boldsymbol{L}$	113.24 mH	Indutance
$\boldsymbol{c}$	1.408 E-5 N.m²/A²	Electromagnet force constant
$\boldsymbol{i_0}$	0.9423 A	Equilibrium current
$\boldsymbol{x_0}$	0.006 m	Air gap equilibrium distance

4. SYSTEM ANALYSES

The stability of the system is evaluated by the analysis of the poles in open loop. After analyzing the stability, the controllability was checked to attest that the system is controllable.

The poles of the system are as follow:

$$\boldsymbol{p} = \begin{bmatrix}+57.18\\ -57.18\\ -52.10\end{bmatrix}$$

The system has a pole with a positive real part, indicating the system instability in open loop. This result is expected since the system would not be able to keep an object in levitation without a control action. The object would naturally fall, or it would join to the core of the electromagnet.

The system controllability is confirmed by the usual test of the controllability matrix, which has rank three.

5. CONTROLLER DESIGN

5.1 *Phase Lead* compensator

Phase lead compensation is a control structure capable of providing stability for the levitation system, improving transient response time and reducing overshoot. Due to these characteristics, it was one of the control techniques adopted in this article. The compensator was synthesized using the root locus method, where the pole and zero positions of the controller were determined so that the dominant closed-loop poles result in the desired performance for the system.

The zero of the controller was positioned on the real axis, close to the stable pole of the system, while a pole, ten times the value of zero was adopted. In this way, the locus of the roots was shifted to the left of the *S* plane. The synthesis of the controller was performed using the *sisotool Matlab* command, which resulted in the controller described below:

$$C(s) = 11.4\ \frac{(s+30)}{(s+300)}. \tag{23}$$

The system was simulated using the nonlinear model of the electromagnetic levitator, to represent the real system more accurately. The system presented stability, however, a large steady-state error was noted.

5.2 *Phase Lead-Lag* compensator

A strategy for systems that present satisfactory transient responses, but present large steady-state errors, consists of adding a second compensator that increases the gain of the open-loop system, without significantly altering the transient response. This benefit can be obtained with a *phase lag* compensator. As expected, there was no significant change in the position of the dominant poles of the closed-loop system by maintaining the pole and zero of the *phase lag* compensator very close to each other. The *phase lead-lag* compensator was synthesized to cause no significant interference in the transient response presented by the *phase lead* compensator. The root locus method was used in the controller synthesis. The controller is described by the following equation:

$$C(s) = 11.4\,\frac{(s+30)(s+1.2)}{(s+300)(s+0.12)}. \tag{24}$$

The *phase lead* and *lead-lag* controllers presented reduced operating ranges compared to the other control techniques considered in this paper. For this reason, the simulations of the *phase lead* and *lead-lag* controllers were carried out separately and the results are shown in Figures 5 and 6.

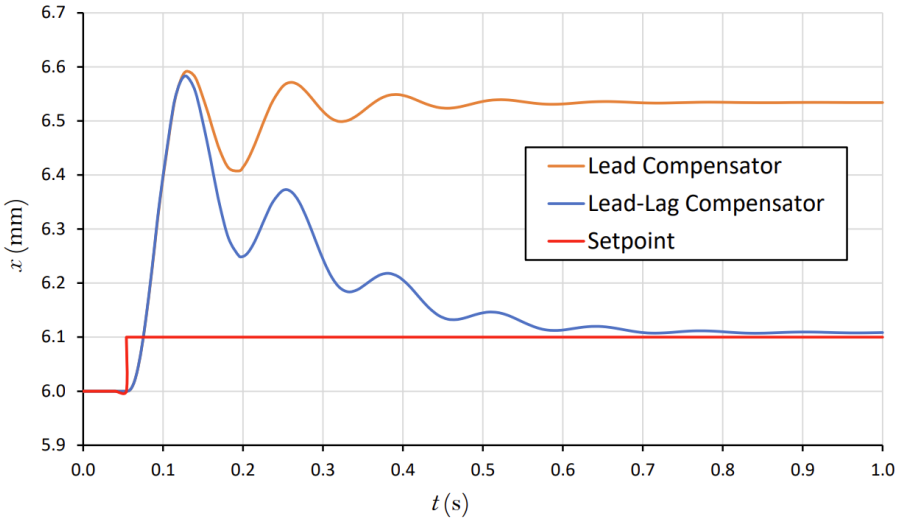

Figure 5. Simulation of *phase lead* and *lead-lag* compensator of the system output.

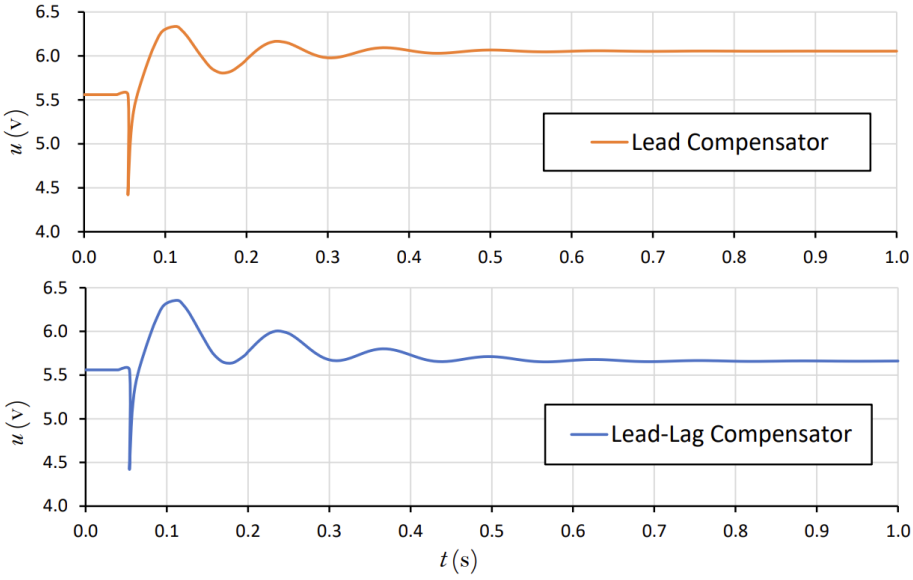

Figure 6. Simulation of *phase lead* and *lead-lag* compensator of the system input.

5.3 *PID control*

PID control is a feedback control system widely used in industrial automation. It adjusts the control action based on a proportional, integral, and derivative terms applied to a tracking error defined by a desired value (Ogata, 2010). The PID control adopted for the system has the following structure:

$$C(s) = k_p + \frac{k_i}{s} + k_d s. \tag{25}$$

where $k_p = 12000$, $k_i = 6000$ and $k_d = 1000$.

5.4 *LQR control*

LQR is an optimal control technique used to design controllers for linear dynamic systems. It aims to minimize a cost function by adjusting control inputs, often employed in applications such as aerospace and robotics (Ogata, 2010). The LQR control adopted here has the following structure:

$$V(t) = Nr(t) - \boldsymbol{K}\boldsymbol{x}(t). \tag{26}$$

where $r(t)$ is the reference, $\boldsymbol{x}(t) = [x(t) \quad v(t) \quad i(t)]^T$ is the state vector, N is a scaling gain of the reference, $\boldsymbol{K}$ is the LQR gain matrix. Considering the linearized model of Eqs. (17) and (18) with weighting matrices for the states and control of $\boldsymbol{Q} = diag(1000,100,0)$ and $R = 1$, we get $N = -927.1$ and $\boldsymbol{K} = [-3909.5 \quad -69.1 \quad 13.1]$.

5.5 *H-Infinity control*

H-Infinity control is a robust control approach used to design controllers that can handle uncertainties and disturbances. It seeks to minimize the maximum gain of the transfer function from disturbances to the controlled output, ensuring robust performance in various engineering applications (Donha, 2006). The H-Infinity control by the mixed sensitive method considering the linearized model with a weighting transfer function for the tracking error of $W_e(s) = 8.3333 \cdot 10^{-5}(s + 0.12)/(s + 0.0015)$ is given by:

$$C(s) = \frac{-1.28\cdot10^{10}s^3 - 1.399\cdot10^{12}s^2 - 3.814\cdot10^{13}s - 5.856\cdot10^{10}}{s^4 + 300.8s^3 + 3.959\cdot10^4 s^2 + 3.185\cdot10^6 s + 3.817\cdot10^5}. \tag{27}$$

The controllers described in sections 5.3, 5.4 and 5.5 were tested in the simulation environment *Matlab Simulink*, and the results are shown in Figures 7 and 8.

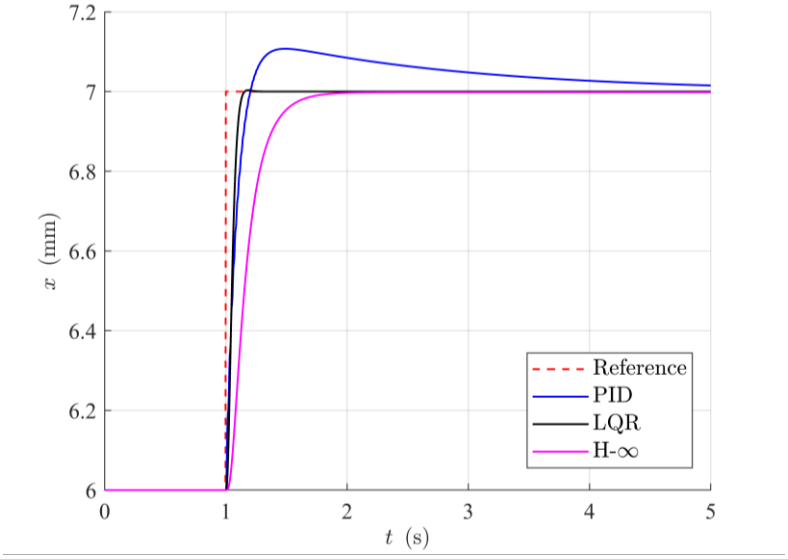

Figure 7. Tracking of PID, LQR and H-Infinity controllers.

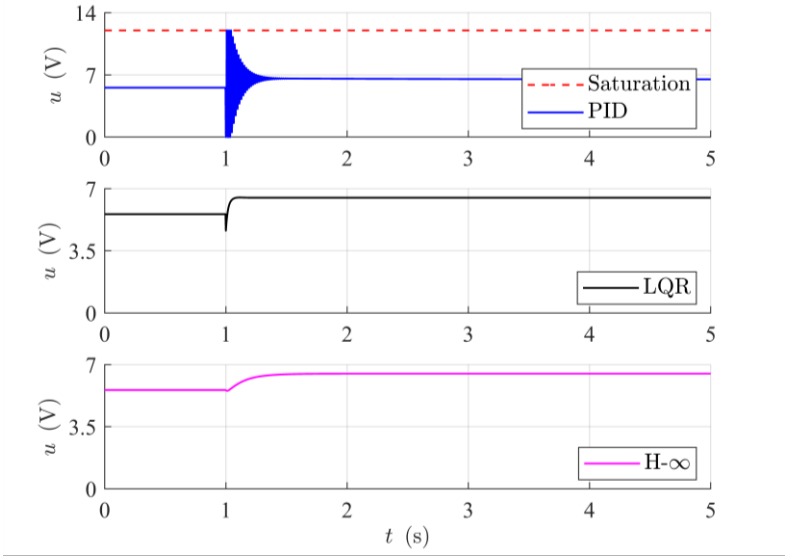

Figure 8. Control input of PID, LQR and H-Infinity controllers.

Figure 7 shows the reference tracking achieved with the other controllers (PID, LQR and H-Infinity). The LQR and H-Infinity presented an improved performance in stabilization and reducing steady state error compared to the PID. Also, the LQR and H-Infinity generated smooth control actions compared to the PID, as seen in Figure 8. The drive voltage calculated by PID presents a high-frequency oscillation at the beginning of the positioning. It reaches the saturation limit of 12 V around the time instant of 1 second. This behavior can compromise the evaluation of PID, generating instabilities during the experiment.

6. EXPERIMENTAL RESULTS

The *phase lead* and *lead-lag* compensators were implemented in the prototype, generating the data presented in Figure 9 and 10.

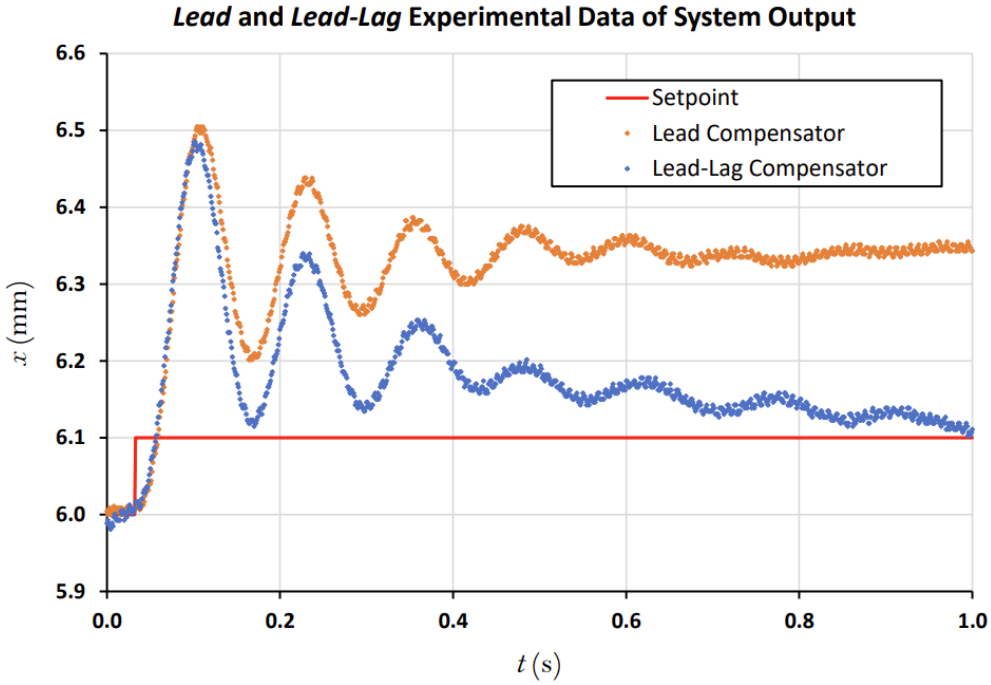

Figure 9. Practical data of the system output.

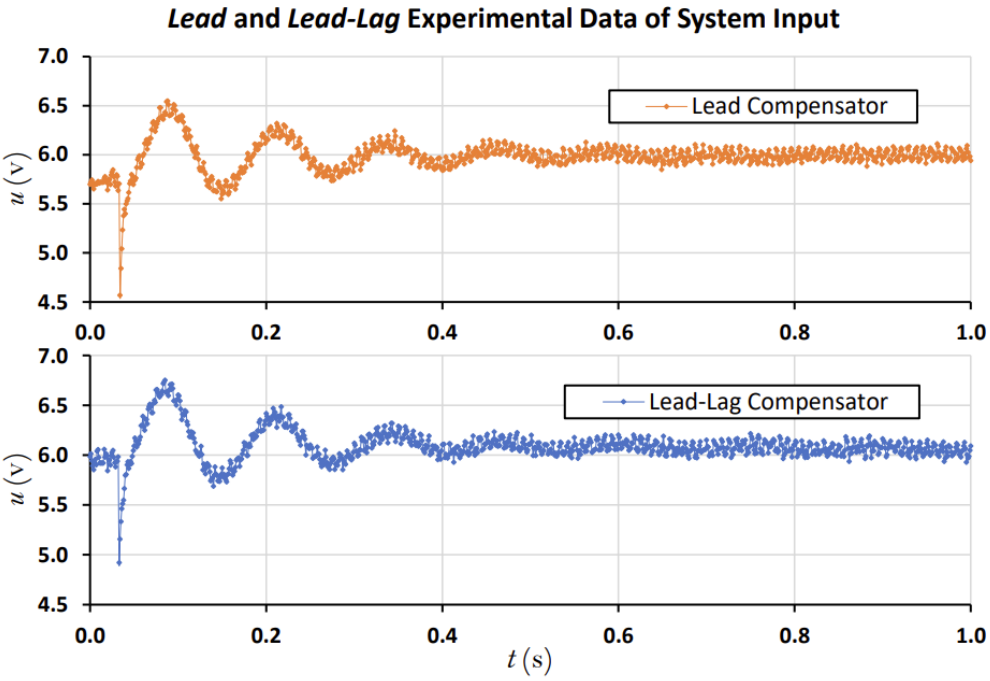

Figure 10. Practical data of the system input.

During the practical experiment, the setpoint was changed from 6.0 mm to 6.1 mm to observe the performance of each controller. The *phase lead* controller stabilizes the system but a steady state error greater than 0.2 mm was observed. To improve the performance of the system in steady state, the *phase lead-lag* controller was synthesized and implemented. As expected, the *phase lead-lag* controller did not significantly change the transient characteristics of the system, however, a great improvement was observed in the system in steady state, considerably reducing the steady state error.

7. CONCLUSION

The application of control techniques in an electromagnetic levitation system by attraction was considered in this paper. To achieve the proposed objectives the system was modeled, linearized and alternative control strategies were implemented. System stability and linearity conditions were verified. The controllers designed using the *lead*, *lead-lag*, PID, LQR and H-Infinity approaches were validated in a simulation environment using the nonlinear mathematical model of the system. To carry out practical checks, a prototype capable of levitating small ferromagnetic objects was built. With the data from the prototype, it was possible to verify the real performance of the system. By implementing *phase lead* and *lead-lag* controllers the system became stable. The presence of a steady state error, slightly greater than 0.3 mm, was observed for the system controlled by *phase lead*, which was considered very high. The performance of the system using the *phase lead-lag* controller was equivalent to the *phase lead* considering the transient characteristics, however, it presented a great improvement considerably reducing the steady state error. For future stages, the PID, LQR and H-Infinity controllers, synthesized and simulated in this work, will be implemented, and subjected to practical verifications and comparisons.

8. REFERENCES

Abubakar, A., Dahiru, I. K., Sulaiman, S. H., & Kunya, A. B., 2019. Robust H-Infinity Control for Magnetic Levitation System. *2019 2nd International Conference of the IEEE Nigeria Computer Chapter (NigeriaComputConf)*, 1–6. https://doi.org/10.1109/NigeriaComputConf45974.2019.8949668

Donha, D. C., 2006. *Teorias Avançadas de Controle*. Universidade de São Paulo.

Goel, A., & Swarup, A., 2016. A novel high-order sliding mode control of magnetic levitation system. *2016 IEEE 59th International Midwest Symposium on Circuits and Systems (MWSCAS)*, *0*(October), 1–4. https://doi.org/10.1109/MWSCAS.2016.7870019

Kumar, P., Malik, S., Toyserkani, E., & Khamesee, M., 2022. Development of an Electromagnetic Micromanipulator Levitation System for Metal Additive Manufacturing Applications. *Micromachines*, *13*(4), 585. https://doi.org/10.3390/mi13040585

Majewski, P., Pawuś, D., Szurpicki, K., & Hunek, W. P., 2022. Toward Optimal Control of a Multivariable Magnetic Levitation System. *Applied Sciences*, *12*(2), 674. https://doi.org/10.3390/app12020674

Ogata, K., 2010. Engenharia de Controle Moderno. In *Modern Control Engineering*. Prentice Hall. https://doi.org/10.1590/S0104-44782009000200010

Yaseen, M. H. A., & Abd, H. J., 2018. Modeling and control for a magnetic levitation system based on SIMLAB platform in real time. *Results in Physics*, *8*, 153–159. https://doi.org/10.1016/j.rinp.2017.11.026

9. RESPONSIBILITY NOTICE

The authors are the only responsible for the printed material included in this paper.